UNCERTAINTIES AND COSMOLOGICAL CONSTRAINTS FROM THE MEGAMASER COSMOLOGY PROJECT

Martine Lokken
Advisor: Dr. Jim Braatz

Department of Astronomy
University of Virginia

This thesis is submitted in partial completion of the requirements of the BS Astronomy-Physics Major.

May 11, 2018

Draft version May 11, 2018
Typeset using LaTeX **modern** style in AASTeX61

UNCERTAINTIES AND COSMOLOGICAL CONSTRAINTS FROM THE MEGAMASER COSMOLOGY PROJECT

Martine Lokken[1] and Jim Braatz[2]

[1] *University of Virginia*
[2] *National Radio Astronomy Observatory*

ABSTRACT

This paper investigates sources of uncertainty within the Megamaser Cosmology Project (MCP) as well as cosmological implications of the results as of 2018. The contribution of uncertainty in the value of the matter energy density parameter, Ω_m, towards total uncertainty on the MCP H_0 calculation is found to be negligible ($< 2\%$) for galaxies at the redshifts currently used by the project. However, if future projects use angular–diameter distances at further redshifts to calculate H_0, the current Planck uncertainty in Ω_m would contribute significantly: it would provide ∼30% of the uncertainty of a 3% H_0 measurement at a redshift of 1. Since peculiar velocity (V_P) uncertainties are another source of error in the H_0 measurement, this study also compares V_P distributions between different types of galaxies in the Illustris simulation. Galaxies identified through their black hole mass range as potential maser hosts show no significant difference in their peculiar velocity distribution than galaxies in different mass ranges. Disk galaxies also do not have a different V_P distribution than ellipticals in the samples tested. The V_P distributions are all approximately Gaussian with standard deviations of ∼200 km/s. Lastly, the current MCP value of $H_0 = 69.3 \pm 4.2$ km/s/Mpc is applied as an external constraint to Cosmic Microwave Background data from the WMAP and Planck probes for open ΛCDM and flat wCDM models. The joint constraints on the Planck data in flat wCDM, for example, are $H_0 = 71.3^{+4.1}_{-3.9}$km/s/Mpc and $w = -1.11^{+0.14}_{-0.13}$ (68% confidence intervals). MCP results currently have larger uncertainties than both the Supernova/Cepheid variable and lensing time-delay methods, and the MCP is consistent with these studies as well as both the Planck and WMAP results.

1. INTRODUCTION

In the last decade, observations of the Cosmic Microwave Background (CMB) from the Wilkinson Microwave Anisotropy Probe (WMAP) and Planck satellites have supported the standard ΛCDM cosmological model. Λ represents the cosmological constant, associated with the accelerating expansion of the universe, while CDM stands for the slow-moving, dissipationless, collisionless Cold Dark Matter which appears to make up the majority of matter in the universe. The angular power spectrum of CMB temperature fluctuations places constraints on the parameters of ΛCDM. However, many parameter combinations are degenerate, such that the CMB data alone can only constrain the pair or group of parameters together but cannot separate and individually constrain each one (Planck Collaboration et al. 2016). Additional information from external measurements of such parameters can break these degeneracies. One important parameter that various projects have attempted to independently determine is the Hubble constant, H_0. However, both the Planck and WMAP values for H_0, when ΛCDM cosmology is assumed, are in conflict with direct H_0 measurements from Type 1a supernovae and Cepheid variable stars (Riess et al. 2016). The Megamaser Cosmology Project seeks to add additional information on this possible tension by providing another direct and independent measurement of H_0 (Gao et al. 2016).

The MCP uses a geometrical method to measure the distance to various galaxies and determine H_0. The project first selects galaxies with strong maser emission from the 22 GHz water molecule transition. These galaxies have Active Galactic Nuclei, so the clouds supplying the maser emission are orbiting a central supermassive black hole. Radio observations are taken over time to determine the velocity and centripetal acceleration of the clouds; then the physical radius is calculated by assuming a Keplerian orbit. In addition, Very Long Baseline Interferometry observations map out the maser distribution on the sky. The comparison of the angular distance between masers in VLBI mapping and the calculated physical radius yields the angular-diameter distance to the galaxy (Reid et al. 2009).

The MCP has thus far determined distances to four galaxies which range from 50 to 150 Mpc away. The value for the Hubble Constant, in its most basic form, comes from the relationship

$$H_0 = v/D, \tag{1}$$

where v is the recessional velocity of the galaxy due only to the Hubble flow and D is its distance. Thus, each galaxy with a distance measurement from the MCP also leads to an independent measurement of H_0. The average value of H_0 from the four galaxies examined thus far is 69.3 ± 4.2 km/s/Mpc (Gao et al. 2016). Ultimately, the project aims to measure distances to ~ 10 galaxies.

This paper first examines two sources of uncertainty in the MCP: prior assumptions of cosmological parameter values and peculiar velocities of the galaxies used. We begin in Section 2 by examining how the existing MCP measurements are dependent on the assumed density parameter of matter, Ω_m. We also extend this calculation to greater distances to determine the redshift for which uncertainty in Ω_m would significantly contribute to uncertainty in H_0.

In Section 3 we examine peculiar velocities in the Illustris simulations to investigate whether they are correlated with various galaxy characteristics. The peculiar velocity (V_P) of a galaxy is its deviation in motion from the Hubble Flow velocity at that distance. Peculiar velocities are difficult to measure, and therefore tend to have a large uncertainty which contributes to that of the recession velocity v (Equation 1) and thus to the total uncertainty in H_0 for each galaxy. To determine whether the assumed uncertainties have been accurate and whether they can be reduced, we test whether V_P distributions of maser galaxies differ from those of a general galaxy sample.

Finally, Section 4 explores the joint constraints on H_0, w and Ω_k when the MCP current result is applied to WMAP9 and Planck 2016 data. w is the equation of state parameter for dark energy which relates its density ρ to pressure P by

$$P = \rho w. \tag{2}$$

For an accelerating universe, $w < -1/3$; for a cosmological constant (Λ), $w = -1$ (Trodden & Carroll 2004). Ω_k is the curvature parameter, which takes the value of 0 for a flat universe. We report the constraints on these parameters for both a flat cosmology where w is allowed to vary, and an open-curvature model where w is fixed to be the cosmological constant.

2. DEPENDENCE OF THE MCP METHOD ON COSMOLOGICAL MODEL ASSUMPTIONS

At small redshifts, the velocity v of a galaxy is related to its redshift z by

$$v \approx cz, \tag{3}$$

where c is the speed of light. However, at large redshifts this becomes inaccurate. As detailed in Hogg (1999), for precision cosmology, velocities should be avoided and a more rigorous definition of H_0 than Equation 1 should be used. Equation 4 holds if the universe has flat cosmology, i.e. $\Omega_k = 0$.

$$H_0 = \frac{c}{D_A(1+z)} \int_0^z \frac{dz'}{E(z')} \tag{4}$$

Therein D_A is the angular diameter distance (which is measured directly from the MCP maser method), and z is the cosmological redshift (due only to the Hubble flow). $E(z)$ is determined by

$$E(z) \equiv [\Omega_M(1+z)^3 + \Omega_\Lambda + \Omega_k(1+z)^2]^{1/2} \tag{5}$$

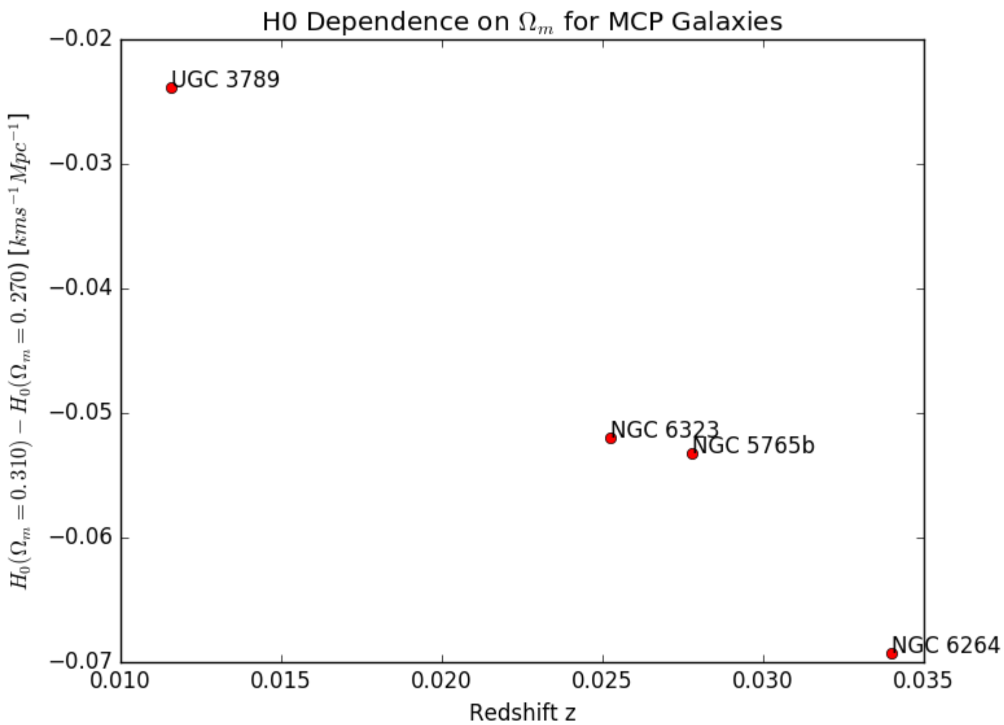

Figure 1. Each red point is a galaxy used in the MCP, plotted at its redshift on the x-axis. On the y-axis is the difference between H_0 calculated with $\Omega_m = 0.31$ and $\Omega_m = 0.27$. The difference is negligible compared to the overall uncertainty of H_0.

The formula for $E(z)$ contains the energy density parameters for matter (Ω_M), dark energy (Ω_Λ), and curvature (Ω_k). The MCP assumes flat (Ω_k=0) geometry and, correspondingly, $\Omega_\Lambda + \Omega_m = 1$. Thus, a value for either Ω_Λ or Ω_m must be chosen for this calculation. Equation 5 shows that at greater redshifts, the calculation of H_0 depends more strongly on the chosen values for Ω_Λ and Ω_M.

While the MCP uses the earlier WMAP result of $\Omega_m = 0.27 \pm 0.04$, the most recent Planck paper reports a measurement of $\Omega_m = 0.310 \pm 0.008$ (Planck Collaboration et al. 2016). The greater precision of the latter value is a product of combining the constraints of Planck with those from Baryon Acoustic Oscillations measurements (BAO). We first test whether the MCP use of the WMAP result rather than Planck significantly affects the H_0 calculation for any of the galaxies used thus far (Figure 1).

Figure 1 demonstrates that the difference in H_0 from using $\Omega_m = 0.27$ versus $\Omega_m = 0.31$ is minor. Even for the most distant galaxy thus far used in the MCP, NGC 6264, this difference is merely 0.07 km/s/Mpc, less than 2% of the total uncertainty on the current combined H_0 measurement (4.2 km/s/Mpc). Given this result, it is safe not to incorporate uncertainties on either Ω_Λ or Ω_m when determining the uncertainty on H_0.

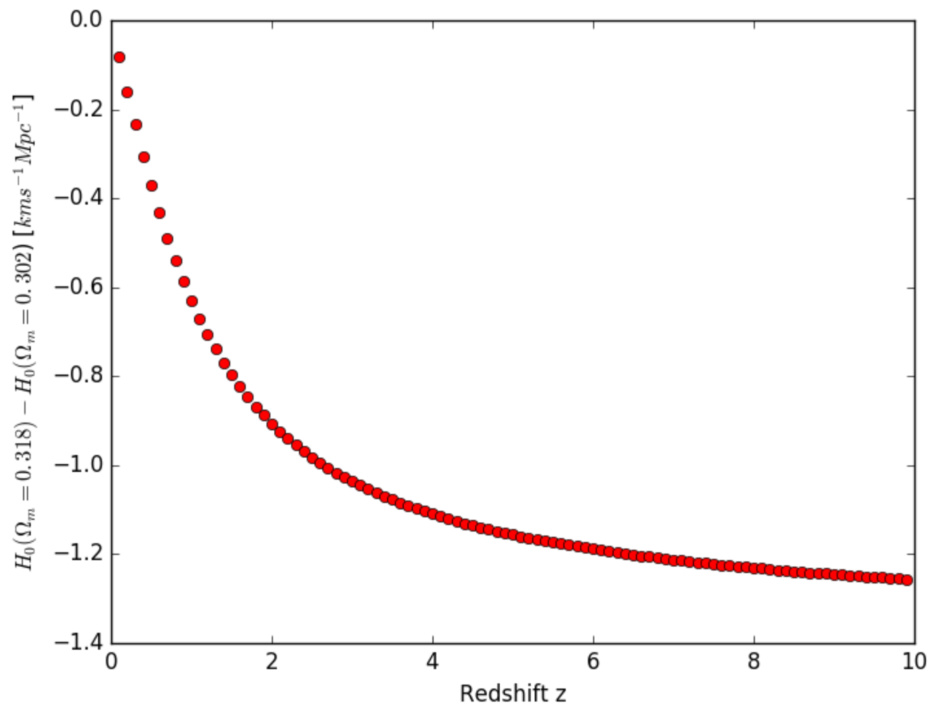

Figure 2. The difference in H_0 when calculated with $\Omega_m = 0.318$ and $\Omega_m = 0.302$, the upper and lower 68% confidence intervals on the Planck result, plotted against redshift. If projects aim to measure H_0 to uncertainties ∼2 km/s/Mpc, and if their methods use angular-diameter distances at redshifts nearing 1 or higher, the cosmological parameter inputs will significantly affect the result.

However, if a group were to measure H_0 using much more distant galaxies and the same methods, the contribution of Ω_m uncertainty would be more significant. Not only would the choice between WMAP results and Planck results be important, but even the uncertainty on an individual Ω_m measurement would need to be folded into total uncertainty. Figure 2 shows the contribution of the uncertainty on Planck's Ω_m value to H_0 measurements at redshifts out to 10. At $z \approx 2$, the difference between using the higher limit and lower limit is about 1 km/s/Mpc. This is significant considering the goal of many such projects is to achieve $\sim 3\%$ accuracy, or around 2 km/s/Mpc uncertainty.

The MCP method of converting an angular-diameter distance into H_0 relies on assumptions about curvature and the energy densities of matter and dark energy. While slight variations in these assumptions do not greatly contribute at small redshifts, if cosmology projects in the future are able to push measurements of D_A to higher redshifts, they need to take those uncertainties into account.

Table 1. Peculiar velocity priors for each of the four MCP galaxies.

Galaxy	Peculiar Velocity [km/s]
UGC 3789	151 ± 163
NGC 6264	0 ± 300
NGC 6323	-285 ± 163
NGC 5765b	0 ± 250

3. PECULIAR VELOCITIES IN THE ILLUSTRIS SIMULATION

The calculation of H_0 in Equation 4 is reliant on the *cosmological* redshift z. However, the *observed* redshift of a galaxy is due not only to its motion from the expansion of the Universe, but also its peculiar velocity. A galaxy's peculiar velocity (V_P) is simply the deviation in its velocity from the smooth Hubble flow, so it differs from the observed velocity V_{obs} by $H_0 D$:

$$V_P = V_{obs} - H_0 D. \tag{6}$$

These deviations from smooth recession come from the inhomogeneous gravitational potentials in the universe; individual galaxy motions are part of larger cosmic flows towards matter overdensities (Masters 2005). For UGC 3789 and NGC 6323, the MCP used a peculiar velocity estimate based on galaxy flow models from the Tully-Fisher relation (Kuo et al. 2015; Reid et al. 2013; Masters et al. 2006). The other two galaxies were assigned a peculiar velocity of 0 and an uncertainty. The values are displayed in Table 1.

Besides the cosmological adjustments discussed in Section 2, the main two sources of uncertainty in H_0 are from the recession velocity and distance measurements (Equation 1). For the closest galaxy, UGC 3789, the uncertainty in its peculiar velocity is only 5% of its recessional velocity (Reid et al. 2013). Meanwhile, its angular-diameter distance was measured to 10%, so the uncertainty in D_A is the main contribution to the total error of H_0. However, as the MCP aims to measure the distance more precisely to $\sim 7\%$ in the future, the peculiar velocity will become a more important contribution and it will be useful to reduce its uncertainty. Thus, we investigate properties of maser galaxy V_P distributions by comparing them to other galaxy types. For this, we turn to the Illustris simulation.

The Illustris simulation (Vogelsberger et al. 2014) is a suite of cosmological simulations performed on a box of 106.5 comoving Mpc per side. The box is evolved from initial conditions at a redshift of 127, with ΛCDM cosmology and WMAP9 results, to present-day. There are three dark-matter-only simulations and three which include both dark matter particles and baryons. The latter are performed using the moving mesh method, with the AREPO code.

During the simulation evolution, structure formation takes place, such that the final present-day solutions mimic our real universe fairly well. At any given redshift, the data[1] identifies "halos", large groups of dark matter particles identified using a Friends-of-Friends algorithm and including also the nearest gas, star, and black hole particles. In the next level down of the structure hierarchy are "subhalos", gravitationally bound substructures within a halo that can include all particle types (dark matter, black holes, gas, and stars). A subhalo could, for example, be analogous to the Milky Way dark matter halo and all its baryonic contents.

We use the Illustris 1 simulation because it is the highest resolution simulation which includes baryons, and therefore its galaxies should be most representative of real galaxy morphologies and kinematics. The Illustris 1 data is composed of 136 snapshots at different redshifts. This study uses Snapshot 133, at redshift 0.024, because the average of the maser galaxies used thus far in the MCP is $\sim$0.025. For the peculiar velocity of a subhalo, we simply use the z direction velocity. At any given redshift snapshot, there is no recession velocity from universe expansion, so the given velocities are all due to local interactions. Since in reality we observe peculiar velocities from some distance, along some line-of-sight, we can arbitrarily choose a direction along which to sample the velocities. The same statistics should result if one were to choose the x or y direction.

To investigate whether peculiar velocities in Illustris are biased by galaxy mass or morphology, we examine different samples of galaxies for similarities and differences. The initial sample includes the 4,000 most massive subhalos in Illustris Snapshot 133. This sample is then reduced to include only those subhalos which are identified as 'central' by the `'primary_flag'`=1 parameter and which contain only one black hole. Galaxies with more than one black hole are currently undergoing a merger in the simulation, and since none of the MCP maser galaxies are in a merger, these are excluded. When the sample is reduced thus, it contains 2,439 subhalos.

We initially break this group into three sub-samples. The first is limited to subhalos containing black holes ranging in mass from 10^6 to $10^8 M_\odot$. This is the mass range for supermassive black holes in the centers of known maser galaxies (Greene et al. 2016), and while limiting black hole mass alone cannot exclusively pick out galaxies likely to host masers, we will call this the 'maser-like' sample for simplicity. This sample includes 2,087 subhalos; more details for all samples are displayed in Table 2. We compare this sample to a high-mass sample, which includes the 500 most massive subhalos in this snapshot. As a third comparison, a sample of low-mass subhalos contains the 500 lowest-mass subhalos from our original 2,439.

The two-sample Kolmogorov-Smirnov (KS) test is a useful statistic for comparing multiple data sets. The test compares two data samples and produces information on the likelihood that they were drawn from the same distribution. If the p-value returned by the test is below a certain threshold, the null hypothesis that the two sets

[1] Publicly accessible at `http://www.illustris-project.org/`.

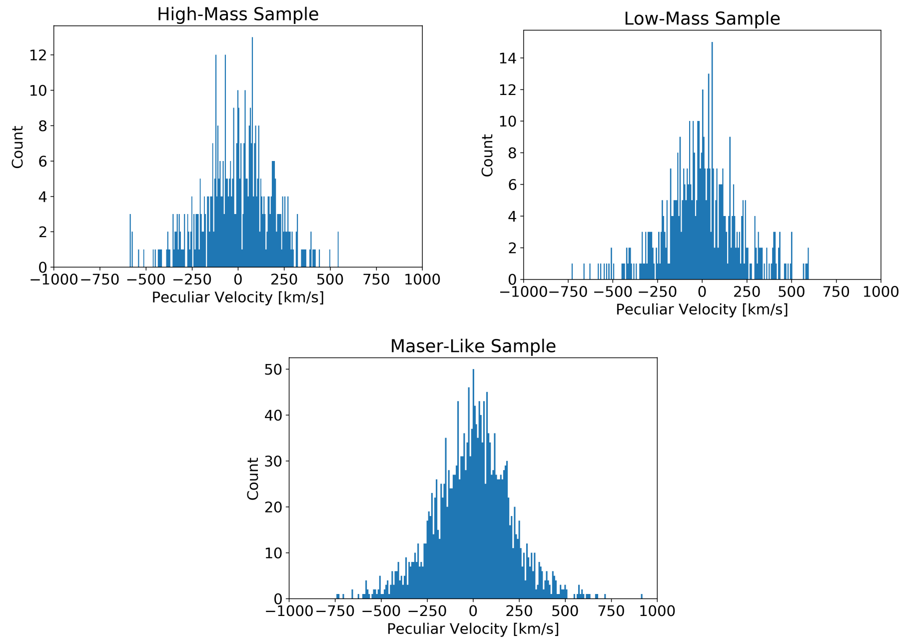

Figure 3. Histograms of the peculiar velocity distributions for the sample of high-mass subhalos, low-mass subhalos, and the maser-like sample. The maser-like sample, since it was only subjected to a cut in black hole masses, has some overlap with both the high-mass and low-mass sample and contains more subhalos than each of the above. Its peculiar velocity distribution is not significantly different than either the high-mass or low-mass subhalos.

were drawn from the same distribution may be rejected. The KS test results from each comparison are shown in Table 3.

Application of the KS-test to the sample of V_P for high-mass galaxies and for maser-like galaxies yields a p-value of 0.84. Comparing the low-mass velocities to the maser-like sample results in a p-value of 0.61. These high p-values mean we cannot say that these samples were drawn from different distributions. Therefore, subhalos with black holes in maser-hosting mass ranges do not significantly differ in peculiar velocity distributions from low-mass or high-mass subhalos, at least in the ranges chosen here. Histograms for each of the three subhalo samples is shown in Figure 3.

However, the low-mass and high-mass samples were least similar, with a p-value of 0.36. The difference is not in the central value of the distribution but in the spread: the standard deviation for the high-mass sample is 191 km/s while that of the low-mass sample is 212 km/s. The reason for this difference may be that the largest subhalos are located at nodes of cosmic flows. They have grown to their size through many past mergers, and these past interactions with other galaxies from various directions have reduced their peculiar velocity in the simulation.

Since masers are so far only found in disk galaxies, we also look for differences in the peculiar velocity distributions of elliptical versus disk galaxies in Illustris. Penoyre et al. (2017) propose multiple methods of dividing Illustris subhalos into these two

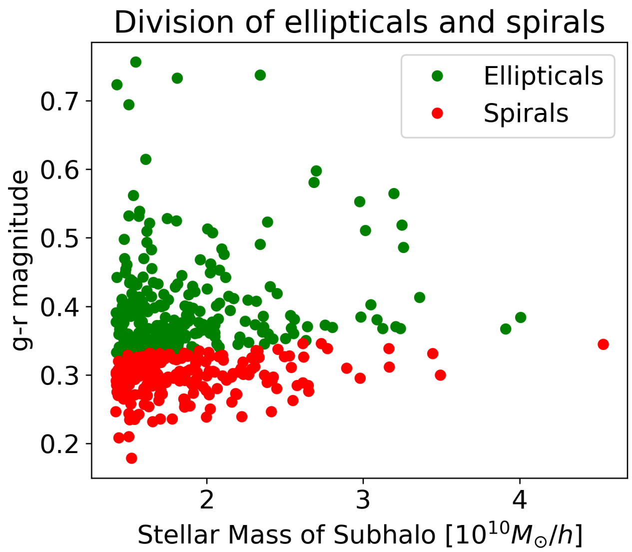

Figure 4. Equation 7 divides the sample of mid-sized subhalos by color into two groups: mostly ellipticals (green) and mostly spirals (red).

morphologies, of which the most straightforward is a color-based division. That work shows that above the line

$$\log_{10}(g - r) = 0.1 \log_{10}(M_*) - 0.5 \tag{7}$$

lie redder, mostly quiescent galaxies, and below lie bluer, star-forming galaxies. Therein g and r are the combined magnitudes of all stars in the subhalo in the g (green) and r (red) SDSS filters, and M_* represents the total stellar mass of the subhalo. This equation divides the Illustris subhalos into the expected fractions of quiescent and star-forming galaxies.

We use this color line to subdivide the original sample of central, single-SMBH galaxies and assume that of the two resulting groups, one contains mostly spiral galaxies and the other mostly ellipticals. To find a similar-sized number of ellipticals and spirals, we cut out the most massive subhalos, which tend to be elliptical. In the reduced sample, there are 199 spirals and 240 ellipticals based on the color cut (Figure 4).

Figure 5 shows the distributions for the peculiar velocities of these samples. The KS test reveals that the peculiar velocities for ellipticals and spirals are similar; the p-value is 0.84. Therefore, at least in this mass range, galaxy morphology has no significant effect on peculiar velocity distribution.

Based on these findings, statistics of peculiar velocities of maser-type galaxies in Illustris are unlikely to differ significantly than statistics of the general galaxy population. The standard deviation of the velocity distributions tends to lie around 200 km/s, which is actually slightly lower than the uncertainties assigned by the MCP to galaxies with no available peculiar velocity information.

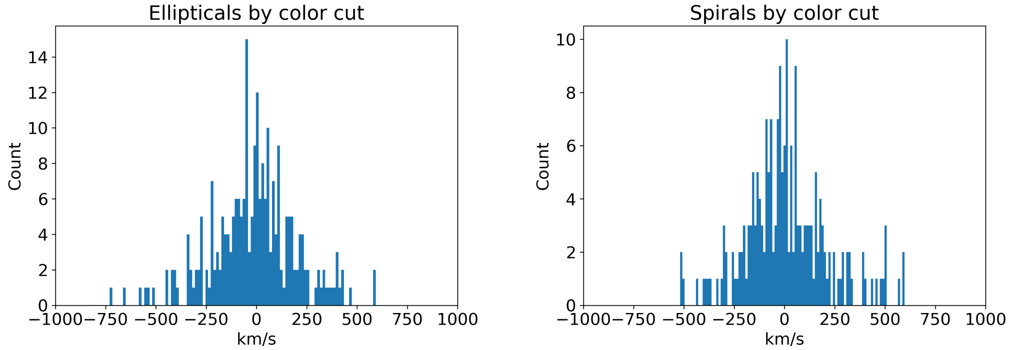

Figure 5. Histograms of the peculiar velocity distributions for the samples of elliptical and spiral subhalos are not significantly different.

Table 2. Details for each of the five samples. The “Mass Range” column represents the total mass of the subhalo, which includes stellar, wind, dark matter, gas, and black hole particles. ‘Mean Velocity’ is the average of the z-direction velocities for the sample.

Sample Type	Mass Range [$10^{10}\mathrm{M}_{\odot}/h$]	Mean Velocity [km/s]	Std. Dev. [km/s]
High-Mass	160 to 1,861	-4.7	191
Low-Mass	14.5 to 47.4	-2.6	212
Maser-Like	14.5 to 420	-3.5	204
Elliptical	14.5 to 45.1	-14.8	213
Spiral	23.1 to 45.2	8.8	207

Table 3. P-values from the KS test comparing different subhalo samples.

Comparison	p-value
High-Mass to Low-Mass	0.36
High-Mass to Maser-Like	0.84
Low-Mass to Maser-Like	0.61
Elliptical to Spiral	0.84

4. APPLICATION OF H_0 AS AN EXTERNAL CONSTRAINT TO W AND Ω_K

The Planck and WMAP satellites, both probes of the Cosmic Microwave Background, have placed constraints on cosmological parameters. The Hubble Constant measured by the MCP provides an external constraint which, when applied to CMB measurements, can break degeneracies between values and improve uncertainties.

We apply the external H_0 measurement for two cosmological models. In the first, flat wCDM, the curvature parameter Ω_k is fixed to 0 and the dark energy parameter w is allowed to vary. In the second, open ΛCDM, w is fixed to -1 (and thus called Λ, the Cosmological Constant) but curvature Ω_k is allowed to vary.

For each model, both the Planck and WMAP teams ran MCMC chains using the COSMOMC program (Lewis 2013) which varied the non-fixed parameters until the set of parameters which best fit the CMB data was found. [2] Each MCMC chain thus results in a probability distribution for the value of each varied parameter. We modify these distributions with the external H_0 measurement by importance sampling the chains.

We use a normalized Gaussian distribution centered at 69.3 with a standard deviation of 4.2 to represent the MCP distribution for H_0. Next, for each value of H_0 sampled by the Planck or WMAP chain, we multiply the weight in the chain by the corresponding weight in the MCP distribution. This results in a modified distribution for each parameter which was varied in that chain. This procedure is applied for both the flat $wCDM$ and open ΛCDM cases.

Following Suyu et al. (2014), for Planck results we use the `plikHM_TT_lowTEB` chains. These represent the statistics of the CMB fluctuations for the baseline high-multipole-moment (high-ℓ) temperature power spectra combined with the low-ℓ temperature and Low Frequency Instrument polarization data.

Figure 6 displays the importance-sampling results. The application of the MCP's independent H_0 measurement breaks the degeneracy between w and H_0 which occurs in CMB data alone, and greatly tightens the constraints on Ω_k in the open geometry case.

The resulting joint constraints are reported below with 68% confidence intervals.

Flat wCDM, WMAP9 + MCP:

$$\begin{cases} H_0 = 69.2^{+4.4}_{-4.2} km/s/Mpc \\ w = -0.96 \pm 0.14 \end{cases}$$

Flat wCDM, Planck 2016 + MCP:

$$\begin{cases} H_0 = 71.3^{+4.1}_{-3.9} km/s/Mpc \\ w = -1.11^{+0.14}_{-0.13} \end{cases}$$

Open ΛCDM, WMAP9 + MCP:

$$\begin{cases} H_0 = 68.8^{+4.5}_{-3.8} km/s/Mpc \\ \Omega_k = 0.0 \pm 0.01 \end{cases}$$

Open ΛCDM, Planck 2016 + MCP:

$$\begin{cases} H_0 = 63.2^{+3.6}_{-3.2} km/s/Mpc \\ \Omega_k = -0.01 \pm 0.01 \end{cases}$$

[2] The Planck parameter chains are publicly available in the full grid of results at `http://pla.esac.esa.int/pla/#cosmology`. This also includes the WMAP 9-year data.

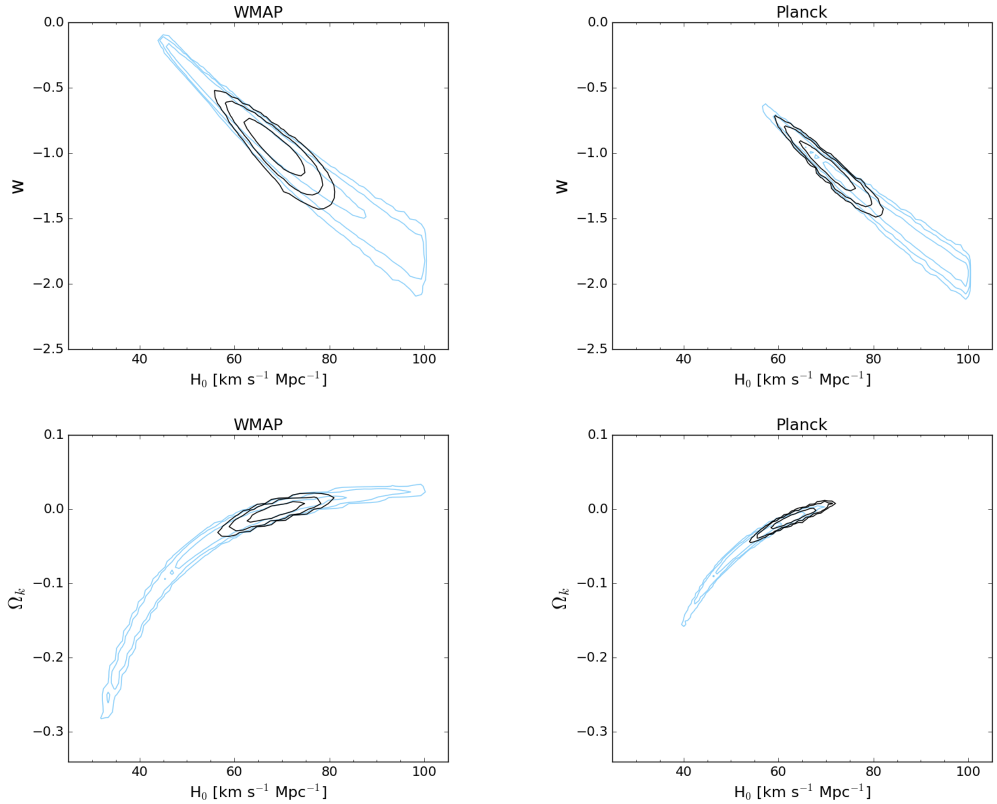

Figure 6. Blue contours surround regions of 68%, 95%, and 99% (1, 2, and 3σ) confidence for the given parameters for WMAP 9-year data (left) and Planck 2015 data (right). The black contours represent the same confidence levels after importance sampling of the CMB data with the MCP H_0 value. The external H_0 measurement, in the case of flat geometry and free w, breaks the degeneracy between w and H_0 (top row). In the case of open geometry and w fixed to the cosmological constant, the H_0 direct measurement greatly increases the constraints on Ω_k (bottom row). The truncated contour edges are due to the Planck or WMAP parameter chain reaching pre-specified upper limits.

Next, we examine how these constraints compare to those placed by other independent H_0 measurements. Riess et al. (2016) uses Cepheid Variable Stars and Type Ia supernovae to measure distances to galaxies, and as of 2016 have determined a value of 73.24 ± 1.74 km s^{-1}Mpc^{-1}. Meanwhile, the H0LiCOW collaboration has thus far analyzed the strong gravitational lensing in three quasar systems, yielding $H_0 = 71.9^{+2.4}_{-3.0}$ km s^{-1}Mpc^{-1} (Bonvin et al. 2017). Figure 7 provides a visualization of the constraints made on w from importance sampling with these relative measurements. Because the Megamaser Cosmology Project has produced a similar H_0 result to each of these values and has not yet reached the precision of the other studies, MCP results neither conflict with nor favor either of them.

5. CONCLUSION

This work has explored multiple sources of uncertainty in the Megamaser Cosmology Project and explored the implications of the project's current results on different cosmological models. The MCP uses a geometrical method to directly determine

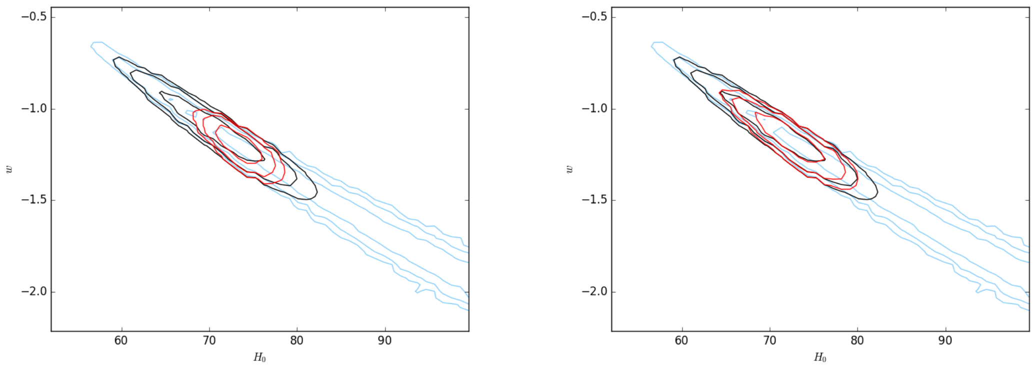

Figure 7. This figure compares the current results of the MCP to those of the distance-ladder and gravitational lensing time-delay methods. Blue contours surround regions of 1, 2, and 3σ confidence for the parameters based on Planck data alone. Black contours represent importance sampling results from the MCP external H_0 measurement, and red contours surround the importance-sampled distribution based on Riess et al. (2016) (left, distance-ladder) and Bonvin et al. (2017) (right, gravitational lensing).

the angular-diameter distance to galaxies; however, calculating the Hubble Constant from this distance requires assumptions about the cosmological model. One such assumption is the value of Ω_m in flat ΛCDM. We have shown that the contribution from Ω_m uncertainty towards overall H_0 error is less than 2% for MCP galaxies (given the correctness of flat curvature). However, if future projects were to extend this geometrical method to much higher redshifts, the contribution could rise to be a significant component of the uncertainty.

Peculiar velocities are another source of uncertainty in calculating H_0. The measured recession velocity for each galaxy is made up of both peculiar motion and motion from the Hubble Flow, but only the latter goes into the calculation for H_0. Therefore, v_P is necessary to extract the latter velocity. For many galaxies, no peculiar velocity is available from observational techniques, so an assumption must be made of the typical distribution and input as uncertainty. An exploration of Illustris subhalos has shown that there is no significant difference between the peculiar velocity distribution of galaxies which have a range of black hole masses within the typical maser range and high- or low-mass samples. Additionally, an approximate color division into elliptical and spiral galaxies also resulted in similar peculiar velocity distributions. The distributions all tended to have a standard deviation of ∼200 km/s, slightly lower than the typical uncertainty input into MCP priors for galaxies without peculiar velocity information.

Lastly, we have used the current MCP results as an external constraint on the WMAP 9–year and Planck 2016 Cosmic Microwave Background data. The additional information breaks the degeneracy between H_0 and w in the CMB data, and greatly narrows the constraints on Ω_k. Compared to the standard candle and gravitational lens time delay methods, the MCP measurement is less precise. However, with a goal of ∼10 additional galaxies being added to the MCP, in the future this project will reach a level of certainty that can help address the possible tensions in the Hubble Constant.

REFERENCES

Bonvin, V., Courbin, F., Suyu, S. H., et al. 2017, MNRAS, 465, 4914

Gao, F., Braatz, J. A., Reid, M. J., et al. 2016, ApJ, 817, 128

Greene, J. E., Seth, A., Kim, M., et al. 2016, ApJL, 826, L32

Hogg, D. W. 1999, ArXiv Astrophysics e-prints, astro-ph/9905116

Kuo, C. Y., Braatz, J. A., Lo, K. Y., et al. 2015, ApJ, 800, 26

Lewis, A. 2013, Phys. Rev., D87, 103529

Masters, K. L. 2005, PhD thesis, Cornell University, New York, USA

Masters, K. L., Springob, C. M., Haynes, M. P., & Giovanelli, R. 2006, ApJ, 653, 861

Penoyre, Z., Moster, B. P., Sijacki, D., & Genel, S. 2017, MNRAS, 468, 3883

Planck Collaboration, Ade, P. A. R., Aghanim, N., et al. 2016, A&A, 594, A13

Reid, M. J., Braatz, J. A., Condon, J. J., et al. 2009, ApJ, 695, 287

—. 2013, ApJ, 767, 154

Riess, A. G., Macri, L. M., Hoffmann, S. L., et al. 2016, ApJ, 826, 56

Suyu, S. H., Treu, T., Hilbert, S., et al. 2014, ApJL, 788, L35

Trodden, M., & Carroll, S. M. 2004, ArXiv Astrophysics e-prints, astro-ph/0401547

Vogelsberger, M., Genel, S., Springel, V., et al. 2014, MNRAS, 444, 1518